Cytosine Detection by a Fluorescein-Labeled Probe Containing Base-Discriminating Fluorescent Nucleobase

Akimitsu Okamoto, Kazuo Tanaka, Tetsuo Fukuta, and Isao Saito*[a]

We report on a new method for the detection of a base at a specific site in a DNA sequence by monitoring the fluorescence emission of fluorescein. To achieve this goal, we developed a new base-discriminating fluorescent (BDF) nucleobase, naphthodeazaadenine (NDA). The fluorescence spectrum of the duplex possessing a cytosine base as a complementary base of NDA showed a fluorescence peak at 383 nm when using an excitation wavelength of 350 nm. When the complementary base of NDA was one of the other bases, the fluorescence intensity was very low. The fluorescence emission spectrum of NDA overlapped with the fluorescence excitation spectrum of fluorescein in the wavelength range of 400–500 nm. Thus, we designed FRET-BDF probes containing NDA as the FRET donor and fluorescein as the acceptor. The interaction of these two fluorophores, which are separated by defined base pairs, allowed an efficient energy transfer that resulted in a dominant fluorescence emission of fluorescein at 520 nm when using an excitation wavelength of 350 nm. Fluorescence emission from FRET-BDF probes was observed only when the complementary base of NDA is C, thus achieving a clear distinction of a C base on the complementary DNA strand. However, the general utility of our method is limited due to the quenching of the NDA fluorescence by a G/C base pair flanking NDA.

Introduction

Fluorescence-labeled nucleic acids are widely used for investigating the structure and dynamics of nucleic acids,[1] and for detecting nucleic acids containing target sequences.[2] At present, a large number of fluorophores, such as fluorescein, TAMRA, JOE, Alexa 594, BODIPY, and cyanine dyes, have been developed, and a variety of analyzers and imagers adjusted to the emission wavelength of these fluorophores are commercially available. However, the fluorescence of these known fluorophores is relatively insensitive to conjugated DNA sequences, with the exception that it is often decreased by a guanine base located in the neighborhood of an attached fluorophore.[3,4] Thus, such fluorophores are unsuitable for direct detection of a small change in DNA microenvironment.

We have recently reported a quite different type of fluorophore, base-discriminating fluorescent (BDF) nucleosides, which can distinguish bases on a complementary DNA strand by the fluorescence change.[5–8] For example, oligodeoxynucleotides (ODNs) containing a synthetic nucleoside benzopyridopyrimidine (BPP), one of the BDF nucleosides developed, selectively emit a strong fluorescence when the complementary base of BPP is A and can be used as an effective BDF probe for the detection of a single nucleotide alteration where an A base is concerned.[5] Such fluorescence behavior of BDF nucleosides has a remarkable advantage that is not observed for the commonly used fluorophores. However, the fluorescence wavelength of the BDF nucleosides is slightly too short to allow the use of commercially available DNA fluorescence analyzers. If the fluorescence wavelength of BDF nucleosides can be shifted to that of conventionally used fluorophores, then the BDF method will become a more powerful tool for the detection of single nucleotide alterations.

Herein, we report on a new method for the detection of a base at a specific site in a DNA sequence by monitoring the fluorescence emission of fluorescein. To achieve this goal, we developed a new BDF nucleobase, naphthodeazaadenine (NDA), which shows a strong fluorescence resonance energy transfer (FRET) emission to fluorescein only when its complementary base is C.

Results and Discussion

The novel BDF nucleoside NDA was synthesized from 2-nitronaphth-1-ol (**1**) (Scheme 1). After condensation with ethyl cyanoacetate, two ring-closure reactions were carried out to afford **5**. Chlorination of **5**, followed by coupling with protected deoxyribose gave **7**. Compound **7** was converted to NDA nucleoside (**8**) by treating it with methanolic ammonia. Subsequently, nucleoside **8** was protected and incorporated via phosphoramidite **11** into the ODNs by using a DNA synthesizer. The NDA-containing and the complementary ODNs used in this study are summarized in Table 1.

Prior to measurements of the fluorescence spectra, the absorption spectra of 2.5 μM of **ODN(NDA)** hybridized with strands containing different bases opposite NDA, **ODN(N)** (N = C, T, G, or A) in sodium phosphate buffer (pH 7.0) were initially meas-

[a] *Dr. A. Okamoto, K. Tanaka, T. Fukuta, Prof. I. Saito*
Department of Synthetic Chemistry and Biological Chemistry
Faculty of Engineering, Kyoto University
and SORST, Japan Science and Technology Corporation
Kyoto 615-8510 (Japan)
Fax: (+81) 75-383-2759
E-mail: saito@sbchem.kyoto-u.ac.jp

  DOI: 10.1002/cbic.200400010 *ChemBioChem* **2004**, *5*, 958 – 963

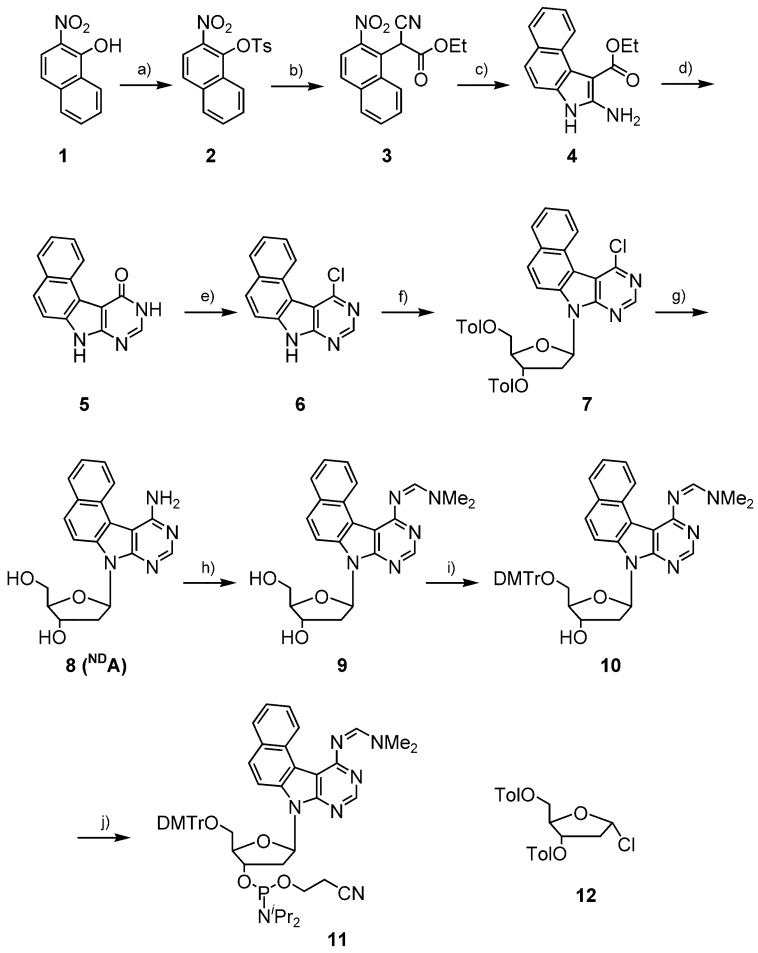

Scheme 1. *Reagents and conditions: a) tosylchloride, pyridine, RT, 6 h, 55%; b) potassium* tert*-butoxide, ethyl cyanoacetate, THF, reflux, 7 h, 65%; c) AcOH, Zn powder, sonication, 44°C, 7 h, 67%; d) sodium methoxide, formamide, 220°C, 6 h, 37%; e) $POCl_3$, p-dioxane, reflux, 3 h, 67%; f) i) sodium hydride, acetonitrile, 55°C, 1 h, ii)* ***12****, RT, 15 min, 86%; g) methanolic ammonia, 150°C, 7 h, 95%; h) DMF dimethylacetal, DMF, RT, 3 h, 66%; i) 4,4′dimethoxytrityl chloride, 4-(dimethylamino)pyridine, pyridine, RT, 4 h, 30%; j) $(iPr_2N)_2PO(CH_2)_2CN$, 1H-tetrazole, acetonitrile, RT, 1.5 h, quant.*

ured (Figure 1). When the complementary base of NDA was G, T, or A, the absorption spectra had their maxima λ_{max} at 352 nm. In contrast, the absorption spectrum given from the **ODN(NDA)/ODN(C)** duplex broadened, and λ_{max} was observed at 354 nm, that is, shifted 2 nm longer than those of the other duplexes.

The fluorescence spectra of **ODN(NDA)** hybridized with **ODN(N)** are shown in Figure 2a. The fluorescence spectrum of the duplex possessing a C base as a complementary base of NDA, **ODN(NDA)/ODN(C)**, showed a fluorescence peak at 383 nm when using an excitation wavelength of 350 nm ($\Phi = 0.027$). In contrast, when the complementary base of NDA was a base other than C, the fluorescence intensity was very low ($\Phi < 0.005$). The fluorescence of **ODN(NDA)/ODN(C)** was approximately nine times stronger than that observed for **ODN(NDA)/ODN(T)**. For single-stranded **ODN(NDA)**, an appreciably strong fluorescence was observed at 378 nm ($\Phi = 0.010$), which was comparable to the peak intensity observed for **ODN(NDA)/ODN(C)**.

The fluorescence character of NDA-containing BDF probes would be useful for the typing of a single nucleotide polymorphism (SNP) where a C base is concerned. For example, a BDF probe **ODN(BRCA-NDA)** was designed for the human breast cancer type 1 gene (BRCA1) sequence, which possesses a C/T SNP site,[9,10] **ODN(BRCA-N)** (N = C or T; Table 1). Upon hybridization with the target sequence, **ODN(BRCA-NDA)** showed an C-allele-specific fluorescence ($\Phi = 0.069$), whereas the fluorescence of **ODN(BRCA-NDA)** hybridized with a T-allele sequence was weak ($\Phi = 0.018$). However, when NDA is flanked by a G/C base pair, its fluorescence is considerably suppressed. When a 15-mer DNA strand containing an angiotensinogen gene C/T SNP site,[9,11] **ODN(AGT-N)** (N = C or T), was used as target sequences, the fluorescence of

Table 1. *Oligodeoxynucleotides used in this study.*

	Sequences
ODN(NDA)	5′-d(CGCAATND**A**TAACGC)-3′
ODN(N)[a]	5′-d(GCGTTA**N**ATTGCG)-3′
ODN(BRCA-NDA)	5′-d(GGTACCAND**A**TGAAATA)-3′
ODN(BRCA-N)[b]	5′-d(TATTTCA**N**TGGTACC)-3′
ODN(AGT-NDA)	5′-d(GGCTCCCND**A**TCAGGGA)-3′
ODN(AGT-N)[b]	5′-d(TCCCTGA**N**GGGAGCC)-3′
ODN(F-3-NDA)[c]	5′-d(**F**AATND**A**TAACGCACACG)-3′
ODN(N-3)[a]	5′-d(CGTGTGCGTTA**N**ATT)-3′
ODN(F-3-A)[c]	5′-d(**F**AATATAACGCACACG)-3′
ODN(3-NDA)	5′-d(AATND**A**TAACGCACACG)-3′
ODN(F-4-NDA)[c]	5′-d(**F**AAATND**A**TAACGCACACG)-3′
ODN(N-4)[a]	5′-d(CGTGTGCGTTA**N**ATTT)-3′
ODN(F-5-NDA)[c]	5′-d(**F**AAAATND**A**TAACGCACACG)-3′
ODN(N-5)[a]	5′-d(CGTGTGCGTTA**N**ATTTT)-3′

[a] "N" denotes C, T, G, and A. [b] "N" denotes C and T. [c] "F" denotes 6-(fluorescein-6-carboxamido)hexanol.

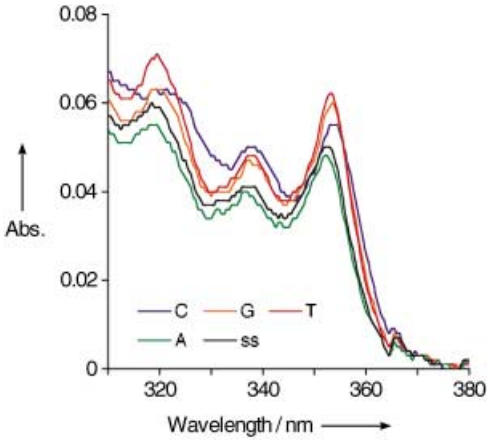

Figure 1. *Absorption spectra of* ***ODN(NDA)*** *(2.5 μM) hybridized with* ***ODN(T)****,* ***ODN(C)****,* ***ODN(G)*** *or* ***ODN(A)*** *(2.5 μM, 50 mM sodium phosphate, 0.1 M sodium chloride, pH 7.0, RT). "ss" denotes single-stranded* ***ODN(NDA)****.*

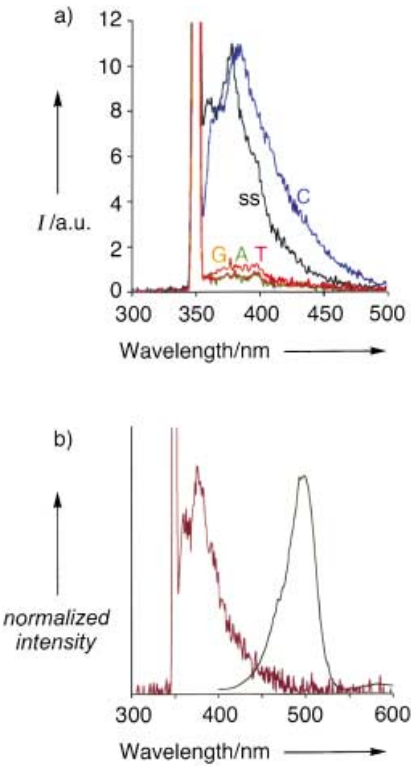

Figure 2. *a) Fluorescence spectra of* ***ODN(*ND*A)*** *(2.5 μM) hybridized with 2.5 μM* ***ODN(T), ODN(C), ODN(G)*** *or* ***ODN(A)*** *(2.5 μM, 50 mM sodium phosphate, 0.1 M sodium chloride, pH 7.0, RT). Excitation wavelength was 350 nm. "ss" denotes single-stranded* ***ODN(*ND*A)****. b) Overlap of an emission spectrum of* ***ODN(3-*ND*A)*** *(purple) and an excitation spectrum of* ***ODN(F-3-A)*** *(green).*

the designed BDF probe **ODN(AGT-NDA)** was very weak, regardless of the nature of the base opposite NDA ($\Phi = 0.003–0.004$). Thus, the C detection method with an NDA-containing probe cannot be used for sequences containing a G/C base pair flanking the SNP site.

The fluorescence emission spectrum of NDA ($\lambda_{em}^{max} = 375$ nm) overlapped with the fluorescence excitation spectrum of fluorescein ($\lambda_{exc}^{max} = 494$ nm) in the wavelength range 400–500 nm (Figure 2b). Thus, the interaction of these two fluorophores, which are separated by defined base pairs, might allow an efficient energy transfer that results in a dominant fluorescence emission of fluorescein at 520 nm when using an excitation wavelength of 350 nm. As shown in Table 1, we designed a series of FRET-BDF probes containing NDA as the FRET donor and fluorescein as the acceptor separated by three (**ODN(F-3-NDA)**), four (**ODN(F-4-NDA)**), or five (**ODN(F-5-NDA)**) A/T base pairs to systematically analyze the fluorescence properties. Initially we investigated the fluorescence properties of the **ODN(F-3-NDA)** FRET-BDF probe. The fluorescence spectra of the **ODN(F-3-NDA)/ODN(N-3)** duplex, measured with various complementary bases of NDA (N), are shown in Figure 3a. The fluorescence emission from **ODN(F-3-NDA)/ODN(N-3)** was observed selectively when N was C. The quenching efficiency (Q_F) of NDA in **ODN(F-3-NDA)/ODN(C-3)** was 83%. The fluorescence lifetime of **ODN(F-3-NDA)/ODN(C-3)** obtained after excitation at 337 nm was 0.59 ns, which was much shorter than that of **ODN(3-NDA)/ODN(C-3)**, which does not possess a FRET acceptor fluorescein (1.10 ns). These observations suggest that effective FRET from NDA to fluorescein occurs in **ODN(F-3-NDA)/ODN(C-3)**. In contrast, the hybridization of **ODN(F-3-NDA)** with **ODN(N-3)** where N is T, G, or A results in a weaker emission, as shown in Figure 3a. These weak fluorescence peaks become negligible after subtraction of the fluorescence spectra of the NDA-free duplex **ODN(F-3-A)/ODN(N-3)** occurring as the background spectrum; this suggests that these weak fluorescence peaks arise from the NDA-independent excitation of fluorescein (Figure 3b). The fluorescence behavior showed that the fluorescence emission of **ODN(F-3-NDA)** by FRET occurs only when the complementary base of NDA is C. In addition, it is noteworthy that the fluorescence in the single-stranded state is effectively suppressed by the use of a FRET system, unlike the strong fluorescence in single-stranded **ODN(NDA)**.

The difference in fluorescence intensities could be detected more conveniently and precisely with a fluorescence imager, as shown in Figure 3c. The sample solutions were illuminated at 312 nm, and the fluorescence images were taken through a 400 nm long pass emission filter (Figure 3c). The fluorescence emission from **ODN(F-3-NDA)/ODN(C-3)** was very strong and clearly distinguishable from the poor fluorescence from the other duplexes. Therefore, the present FRET-BDF probe method that makes use of the interaction between NDA and

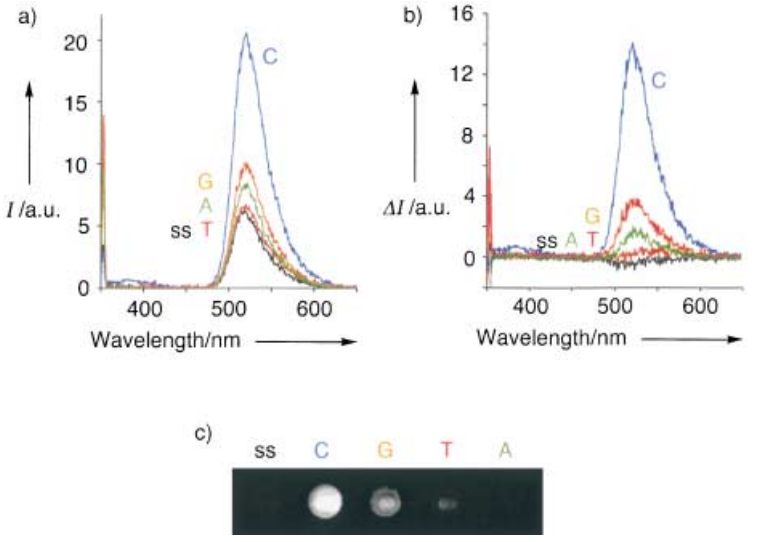

Figure 3. *a) Fluorescence spectra of* ***ODN(F-3-NDA)*** *(2.5 μM) hybridized with* ***ODN(T-3), ODN(C-3), ODN(G-3)*** *or* ***ODN(A-3)*** *(2.5 μM, 50 mM sodium phosphate, 0.1 M sodium chloride, pH 7.0, RT). Excitation wavelength was 350 nm. "ss" denotes single-stranded* ***ODN(F-3-NDA)****. b) The spectra given by subtracting fluorescence spectra of* ***ODN(F-3-A)*** *(2.5 μM) hybridized with* ***ODN(T-3), ODN(C-3), ODN(G-3)*** *or* ***ODN(A-3)*** *(2.5 μM) from spectra (a). c) Fluorescence image of* ***ODN(F-3-NDA)*** *(2.5 μM) hybridized with* ***ODN(T-3), ODN(C-3), ODN(G-3)*** *or* ***ODN(A-3)*** *(2.5 μM, 50 mM sodium phosphate, 0.1 M sodium chloride, pH 7.0, RT). The sample solutions were illuminated with a 312 nm transilluminator. The image was taken through a 400 nm long pass emission filter. "ss" denotes single-stranded* ***ODN(F-3-NDA)****.*

fluorescein constitutes a powerful tool for typing single-nucleotide alterations where a C base is concerned.

To further analyze the character of the FRET interaction through NDA in detail, we examined the fluorescence properties of **ODN(F-4-NDA)/ODN(C-4)**, in which two fluorophores are separated by four A/T base pairs, and compared the fluorescence to that from **ODN(F-3-NDA)/ODN(C-3)** (Table 2). The fluorescence quenching efficiency of NDA in **ODN(F-4-NDA)/ODN(C-4)** was 66%, which is much lower than that observed for **ODN(F-3-NDA)/ODN(C-3)**. The decrease in FRET efficiency also appeared in the fluorescence decay profile of **ODN(F-4-NDA)/ODN(C-4)**. The fluorescent decay profile of **ODN(F-4-NDA)/ODN(C-4)** was fitted to a biexponential function. The major short-lived component, which corresponded to the FRET quenching of NDA, had an extended lifetime, and a new longer-lifetime component, which corresponded to the quenching of NDA itself, appeared. This observation clearly shows the decrease in the efficiency of the FRET from NDA to fluorescein. The lowering of this FRET efficiency had a serious effect on the complementary-base selectivity in the fluorescence emission of fluorescein. As clearly seen in Table 2, a remarkable decrease in C selectivity in the fluorescence emission was observed in **ODN(F-4-NDA)/ODN(C-4)**. The decrease in FRET efficiency was more marked in the duplex in which the two fluorophores were more separated (**ODN(F-5-NDA)/ODN(C-5)**). The Q_F of **ODN(F-5-NDA)/ODN(C-5)** decreased to 48%, and the C selectivity in the fluorescence emission was approximately half that of **ODN(F-3-NDA)/ODN(C-3)**. The results of these fluorescence measurements for a series of fluorescence-labeled ODNs imply that the FRET efficiency between NDA as a FRET donor and fluorescein as an acceptor is strongly correlated with the complementary base selectivity in the fluorescence emission of fluorescein.

Table 2. *Fluorescence data of FRET-BDF probes.*

	τ_1 [ns] (%)	τ_2 [ns] (%)	τ_M [ns]	Q_F[a]	C/T/ss ratio[b]
ODN(F-3-NDA)/ODN(C-3)	0.589		0.589	0.829	3.1:1.0:0.9
ODN(F-4-NDA)/ODN(C-4)	0.625 (98)	3.033 (2)	0.673	0.663	2.1:1.0:1.1
ODN(F-5-NDA)/ODN(C-5)	0.630 (97)	2.209 (3)	0.677	0.482	1.8:1.0:1.2
ODN(3-NDA)/ODN(C-3)		1.103	1.103	–	9.5:1.0:8.6[c]

[a] Q_F is the quenching efficiency for NDA. [b] The C/T/ss ratio shows the ratio of the fluorescence intensities of fluorescein (521 nm) from NDA/C duplexes, NDA/T duplexes, and single-stranded ODNs. [c] The ratio of the fluorescence intensities of NDA (376 nm) from NDA/C duplexes, NDA/T duplexes, and single-stranded ODNs.

Conclusion

In conclusion, it has been possible to clearly distinguish the presence of a cytosine base on a complementary DNA strand by using FRET-BDF probes. By using FRET-BDF probes that contain both NDA and fluorescein, the complementary base-selective fluorescence of NDA was transferred to fluorescein. This system facilitates the detection of a single-nucleotide alteration in a target sequence at the wavelength of fluorescein emission. However, our method cannot be used if the sequence containing a G/C base pair that flanks the NDA, because the fluorescence of NDA is then quenched.

Experimental Section

General: ^{1}H NMR spectra were measured on a Varian Mercury 400 (400 MHz) spectrometer. Coupling constants are reported in hertz. The chemical shifts are expressed in ppm downfield from tetramethylsilane, with residual chloroform ($\delta = 7.24$) and dimethylsulfoxide ($\delta = 2.48$) as internal standards. FAB mass spectra were recorded on a JEOL JMS DX-300 or JMS SX-102A spectrometer.

2-nitronaphthyl *p*-toluenesulfonate (2): 2-Nitronaphth-1-ol (**1**; 95%, 10.0 g, 50.1 mmol) was dissolved in pyridine (150 mL), and *p*-toluenesulfonyl chloride (12.0 g, 62.9 mmol) was added at 0°C. The mixture was stirred at room temperature for 6 h, then concentrated in vacuo. The crude product was purified by silica gel chromatography with chloroform to give **2** (9.4 g, 27.4 mmol, 55%) as an orange solid. ^{1}H NMR ($CDCl_3$) $\delta = 8.18$ (d, $J = 8.8$ Hz, 1H), 7.84–7.94 (5H), 7.67 (ddd, $J = 8.8$, 7.2, 1.2 Hz, 1H), 7.59 (ddd, $J = 8.8$, 7.2, 1.2 Hz, 1H), 7.37 (d, $J = 8.8$ Hz, 2H), 2.49 (s, 3H); MS (FAB) (NBA/$CDCl_3$): *m/z*: 343 $[M]^+$; HRMS (FAB) calcd for $C_{17}H_{13}O_5NS$: 343.0514 $[M]^+$, found 343.0514.

Cyano(2-nitronaphthalene-1-yl)acetic acid ethyl ester (3): Potassium *tert*-butoxide (4.78 g, 42.6 mmol) was added to an ice-cold solution of ethyl cyanoacetate (4.62 mL, 42.6 mmol) in anhydrous THF (170 mL). The suspension formed was stirred for 15 min, then treated with **2** (7.3 g, 21.3 mmol) and heated at reflux for 7 h. The solution was poured into water, and the aqueous mixture was acidified to pH 2 with concentrated HCl. The mixture was extracted with ether (3×), and then the combined organic phases were dried and concentrated in vacuo. The crude product was purified by silica gel chromatography (chloroform/methanol 10:1) to give **3** (3.7 g, 13.8 mmol, 65%) as a yellow solid. ^{1}H NMR ([D_6]DMSO) $\delta = 8.43$ (d, $J = 8.4$ Hz, 1H), 8.34 (d, $J = 9.2$ Hz, 1H), 8.23 (m, 1H), 8.14 (d, $J = 9.2$ Hz, 1H), 7.87 (m, 2H), 6.87 (s, 1H), 4.22 (dq, $J = 7.2$, 1.2 Hz, 2H), 1.18 (t, $J = 7.2$ Hz, 3H).

3,11-Dihydro-benzo[*e*]pyrimido[4,5-*b*]indol-4-one (5): A solution of **3** (3.7 g, 13.8 mmol) in acetic acid (150 mL) was treated with a single charge of Zn dust (3.9 g, 60 mmol). The mixture was heated at 44°C and sonicated for 3.3 h, then treated with more Zn (2.4 g, 36.7 mmol). After being heated and sonicated for another 3.3 h, the mixture was filtered. The filtrate was concentrated in vacuo. The crude product was purified by silica gel chromatography (chloroform/methanol 20:1) to give **4** (2.34 g, 9.2 mmol, 67%) as a black solid. MS (FAB) (NBA): *m/z*: 254 $[M]^+$; HRMS (FAB) calcd for $C_{15}H_{14}O_2N_2$: 254.1055 $[M]^+$, found 254.1056. Subsequently, a solution of **4** (1.1 g, 4,33 mmol), sodium methoxide (1.0 g, 18.5 mmol), and formamide (40 mL) was heated at 220°C for 6 h and distilled at 220°C to a solid. The solid was triturated in methanol and then filtered. The filtrate was concentrated to a solid. The crude product was purified by silica gel chromatography (chloroform/methanol 10:1) to give **5** (379 mg, 1.61 mmol, 37%) as a yellow solid. ^{1}H NMR ([D_6]DMSO) $\delta = 12.63$ (s, 1H), 12.29 (s, 1H), 9.93 (d, $J = 8.0$ Hz, 1H), 8.13 (s, 1H), 7.96 (d, $J = 8.0$ Hz, 1H) 7.83 (d, $J = 8.8$ Hz, 1H), 7.65 (d, $J = 8.8$ Hz, 1H) 7.57 (t, $J = 8.8$ Hz, 1H) 7.44 (t, $J =$

8.8 Hz, 1H); MS (FAB) (NBA): *m/z*: 235 $[M]^+$; HRMS (FAB) calcd for $C_{14}H_9ON_3$: 235.0746 $[M]^+$, found 235.0746.

4-Chloro-11*H*-benzo[*e*]pyrimido[4,5-*b*]indole (6): A mixture of **5** (200 mg, 0.85 mmol), $POCl_3$ (20 mL), and *p*-dioxane (20 mL) was heated at reflux for 3 h. The mixture was concentrated to solid, then washed with water. The crude product was purified by silica gel chromatography (chloroform/methanol 40:1) to give **6** (145 mg, 0.57 mmol, 67%) as a yellow solid. ^{1}H NMR ([D$_6$]DMSO) δ = 13.31 (s, 1H), 9.55 (d, J = 8.4 Hz, 1H), 8.78 (s, 1H), 8.15 (d, J = 8.8 Hz, 1H), 8.11 (d, 8.4 Hz, 1H), 7.79 (d, J = 8.8 Hz, 1H), 7.23 (t, J = 8.4 Hz, 1H); MS (FAB) (NBA/DMSO): *m/z*: 254 $[M+H]^+$; HRMS (FAB) calcd for $C_{14}H_8ClN_3$: 254.0485 $[M+H]^+$, found 254.0487.

4-Chloro-11-(2′-deoxy-3′,5′-di-*O*-*p*-toluoyl-β-D-*erythro*-pentofuranosyl)-11*H*-benzo[*e*]pyrimido[4,5-*b*]indole (7): Compound **6** (112 mg, 0.44 mmol) was suspended in dry acetonitrile (10 mL) at room temperature. Sodium hydride (60% in oil; 19.2 mg, 0.48 mmol) was added to this suspension, and the mixture was stirred at 55 °C for 1 h. More sodium hydride (37 mg, 0.93 mmol) was then added, and the mixture was stirred at 55 °C for 30 min. Compound **12** (184 mg, 0.47 mmol) was added, and the mixture was stirred for 15 min, then evaporated to dryness, and the residue was purified by silica gel chromatography (chloroform/methanol 10:1) to give **7** (234 mg, 0.38 mmol, 86%) as a yellow solid. ^{1}H NMR ($CDCl_3$) δ = 9.62 (d, J = 9.2 Hz, 1H), 8.76 (s, 1H), 7.99–8.03 (m, 6H), 7.89 (d, J = 8.0 Hz, 1H), 7.70 (t, J = 8.0 Hz, 1H) 7.64 (d, J = 8.8 Hz, 1H), 7.54 (t, J = 7.2 Hz, 1H), 7.31 (d, J = 8.0 Hz, 2H), 7.24–7.27 (2H), 6.00 (m, 1H), 4.93 (dd, J = 12.0, 3.2 Hz, 1H), 4.77 (dd, J = 12.0, 4.0 Hz, 1H), 4.64 (dd, J = 7.2, 4.0 Hz, 1H), 3.56 (m, 1H), 2.65 (ddd, J = 8.0, 6.4, 2.8 Hz, 1H) 2.46 (s, 6H); MS (FAB) (NBA/$CHCl_3$): *m/z*: 606 $[M+H]^+$; HRMS (FAB) calcd for $C_{35}H_{28}ClN_3O_8$: 606.1796 $[M+H]^+$, found 606.1795.

4-Amino-11-(2′-deoxy-β-D-*erythro*-pentofuranosyl)-11*H*-benzo[*e*]-pyrimido[4,5-*b*]indole (8, NDA): A suspension of **7** (101 mg, 0.167 mmol) in methanolic ammonia (40 mL, saturated at −76 °C) was stirred at 150 °C in a sealed bottle for 7 h. The mixture was evaporated to dryness, and the residue was purified by silica gel chromatography (chloroform/methanol 10:1) to give **8** (55.6 mg, 0.158 mmol, 95%) as a white solid. ^{1}H NMR ([D$_6$]DMSO) δ = 8.77 (d, J = 8.8 Hz, 1H), 8.33 (s, 1H), 8.16 (d, J = 8.8 Hz, 1H), 8.05 (d, J = 8.8 Hz, 1H), 7.93 (d, J = 8.8 Hz, 1H), 7.65 (t, J = 8.8 Hz, 1H), 7.45 (t, J = 8.8 Hz, 1H), 7.07 (s, 2H), 6.99 (t, J = 7.6 Hz, 1H), 5.35 (d, J = 4.0 Hz, 1H), 5.23 (t, J = 5.2 Hz, 1H), 4.52 (m, 1H), 3.91 (d, J = 3.2 Hz, 1H), 3.74 (m, 1H), 3.70 (m, 1H), 2.90 (m, 1H), 2.11 (ddd, J = 8.8, 6.4, 2.0 Hz, 2H); MS (FAB) (NBA): *m/z*: 351 $[M+H]^+$; HRMS (FAB) calcd for $C_{19}H_{19}O_3N_4$: 351.1457 $[M+H]^+$, found 351.1449.

4-(*N*,*N*′-Dimethylaminomethylidenyl)amino-11-(2′-deoxy-β-D-*erythro*-pentofuranosyl)-11*H*-benzo[*e*]pyrimido[4,5-*b*]indole (9): A solution of **8** (55.6 mg, 0.158 mmol) and *N*,*N*-dimethylformamide dimethylacetal (5 mL, 28 mmol) in dimethylformamide (5 mL) was stirred for 3 h at room temperature, then the solvent was concentrated in vacuo. Silica gel chromatography (chloroform/methanol 10:1) yielded **9** (42.5 mg, 0.105 mmol, 66%) as a yellow solid. ^{1}H NMR ([D$_6$]DMSO) δ = 10.90 (d, J = 8.4 Hz, 1H) 9.03 (s, 1H), 8.53 (s, 1H), 8.18 (d, J = 8.4 Hz, 1H), 7.99 (d, J = 8.0 Hz, 1H), 7.93 (d, J = 8.0 Hz, 1H), 7.58 (t, J = 8.0 Hz, 1H), 7.46 (t, J = 8.0 Hz, 1H), 7.05 (t, J = 7.2 Hz, 1H), 5.37 (d, J = 5.2 Hz, 1H), 5.25 (t, J = 5.6 Hz, 1H), 4.53 (m, 1H), 3.91 (m, 1H), 3.72 (m, 2H), 2.92 (m, 1H), 2.11 (m, 1H); MS (FAB) (NBA/$CDCl_3$): *m/z*: 406 $[M+H]^+$; HRMS (FAB) calcd for $C_{22}H_{24}O_3N_5$: 406.1879 $[M+H]^+$, found 406.1882.

4-(*N*,*N*′-Dimethylaminomethylidenyl)amino-11-(2′-deoxy-5′-*O*-dimethoxytrityl-β-D-*erythro*-pentofuranosyl)-11*H*-benzo[*e*]pyrimido[4,5-*b*]indole (10): A solution of **9** (42.5 mg, 0.104 mmol), 4,4′-dimethoxytrityl chloride (46.0 mg, 0.135 mmol), and 4-dimethylaminopyridine (3.1 mg, 0.026 mmol) in anhydrous pyridine (15 mL) was stirred for 4 h at room temperature. The solvent was concentrated in vacuo to a brown oil. The crude product was purified by silica gel chromatography (chloroform/methanol 10:1) to give **10** (22 mg, 0.031 mmol, 30%) as a white solid. ^{1}H NMR ($CDCl_3$) δ = 10.82 (d, J = 8.4 Hz, 1H), 8.87 (s, 1H), 8.57 (s, 1H), 8.07 (d, J = 8.8 Hz, 1H), 7.83 (d, J = 7.2 Hz, 1H), 7.55–7.15 (m, 12H), 6.77 (d, J = 8.4 Hz, 4H), 4.95–4.91 (m, 1H), 4.10 (ddd, J = 4.0 Hz, 1H), 3.54 (dq, J = 25.6, 4.0 Hz, 2H), 3.73 (s, 6H), 3.44 (s, 6H), 3.26 (s,1H), 2.36 (s, 1H).

4-(*N*,*N*′-Dimethylaminomethylidenyl)amino-11-(2′-deoxy-5′-*O*-dimethoxytrityl-β-D-*erythro*-pentofuranosyl-3′-*O*-cyanoethyl-*N*,*N*′-diisopropylphosphoramidite)-11*H*-benzo[*e*]pyrimido[4,5-*b*]indole (11): A solution of **10** (22 mg, 0.031 mmol), 2-cyanoethyl tetraisopropylphosphorodiamidite (10.75 mL, 0.034 mmol), and tetrazole (2.38 mg, 0.034 mmol) in acetonitrile (0.40 mL) was stirred at room temperature for 1.5 h. The mixture was filtered and used for ODN synthesis with no further purification.

Modified ODN synthesis: The modified ODNs were synthesized by a conventional phosphoramidite method with an Applied Biosystems 392 DNA/RNA synthesizer. Synthesized ODNs were purified by reverse-phase HPLC on a 5-ODS-H column (10×150 mm, elution with a solvent mixture of triethylammonium acetate (0.1 M, TEAA), pH 7.0, linear gradient over 30 min from 5% to 20% acetonitrile at a flow rate 3.0 mL min^{-1}). Mass spectra of ODNs purified by HPLC were determined with a MALDI-TOF mass spectroscopy (acceleration voltage 21 kV, negative mode) with 2′,3′,4′-trihydroxyacetophenone (THAP) as matrix and T_8 ($[M-H]^-$ 2370.61) and T_{17} ($[M-H]^-$ 5108.37) as internal standards.

ODN(NDA): MALDI-TOF $[M-H^-]$ calcd: 4025.72, found: 4026.37. **ODN(BRCA-NDA)** MALDI-TOF $[M-H^-]$ calcd: 4707.17, found: 4706.16; **ODN(AGT-NDA)** MALDI-TOF $[M-H^-]$ calcd: 4675.10, found: 4676.98; **ODN(F-3-NDA)** MALDI-TOF $[M-H^-]$ calcd: 5189.59, found: 5190.14; **ODN(3-NDA)** MALDI-TOF $[M-H^-]$ calcd: 4652.14, found: 4651.62; **ODN(F-4-NDA)** MALDI-TOF $[M-H^-]$ calcd: 5502.80, found: 5503.86; **ODN(F-5-NDA)** MALDI-TOF $[M-H^-]$ calcd: 5816.01, found: 5817.27.

Fluorescence measurements: All the fluorescence spectra of the DNA duplexes were taken at room temperature in a buffer solution (pH 7.0) containing sodium phosphate buffer (50 mM) and sodium chloride (100 mM). The fluorescence spectra were obtained by using a SHIMADZU RF-5300PC spectrofluorophotometer; path length = 1 cm, bandwidth = 1.5 nm. Fluorescence imaging was performed by using a Bio-Rad VersaDoc 3000 imaging system. The sample solutions were illuminated with a 312 nm transilluminator. The image was taken through a 400 nm long pass emission filter.

Fluorescence decay measurements: Fluorescence decay was measured by a two-dimensional photon-counting method with the picosecond fluorescence lifetime measurement system (C4780, Hamamatsu). A N_2 laser (337 nm) was used as the excitation light source. The fluorescence emission was collected at 380 nm.

Keywords: DNA · fluorescence resonance energy transfer · fluorescent probes · nucleobases · single-nucleotide polymorphism

[1] D. P. Millar, *Curr. Opin. Struct. Biol.* **1996**, *6*, 322–326.
[2] A. N. Glazer, R. A. Mathies, *Curr. Opin. Biotechnol.* **1997**, *8*, 94–102.

[3] I. Nazarenko, R. Pires, B. Lowe, M. Obaidy, A. Rashtchian, *Nucleic Acids Res.* **2002**, *30*, 2089 – 2095.
[4] S. A. E. Marras, F. R. Kramer, S. Tyagi, *Nucleic Acids Res.* **2002**, *30*, e122.
[5] A. Okamoto, K. Tainaka, I. Saito, *J. Am. Chem. Soc.* **2003**, *125*, 4972 – 4973.
[6] A. Okamoto, K. Tainaka, I. Saito, *Chem. Lett.* **2003**, *32*, 684 – 685.
[7] A. Okamoto, K. Tanaka, T. Fukuta, I. Saito, *J. Am. Chem. Soc.* **2003**, *125*, 9296 – 9297.
[8] A. Okamoto, K. Tainaka, I. Saito, *Tetrahedron Lett.* **2003**, *44*, 6871 – 6874.
[9] H. Haga, Y. Yamada, Y. Ohnishi, Y. Nakamura, T. Tanaka, *J. Hum. Genet.* **2002**, *47*, 605 – 610.
[10] http://snp.ims.u-tokyo.ac.jp/cgi-bin/SnpInfo.cgi?SNP_ID=IMS-JST005851.
[11] http://snp.ims.u-tokyo.ac.jp/cgi-bin/SnpInfo.cgi?SNP_ID=IMS-JST050962.

Received: January 15, 2004

